Vis Comput
DOI 10.1007/s00371-011-0668-6

ORIGINAL ARTICLE

A gradient-domain-based edge-preserving sharpen filter

Zhi-Feng Xie · Rynson W.H. Lau · Yan Gui · Min-Gang Chen · Li-Zhuang Ma

Abstract As one of the most fundamental operations in computer graphics and computer vision, sharpness enhancement can enhance an image in respect of sharpness characteristics. Unfortunately, the prevalent methods often fail to eliminate image noise, unrealistic details, or incoherent enhancement. In this paper, we propose a new sharpness enhancement approach that can boost the sharpness characteristics of an image effectively with affinity-based edge preserving. Our approach includes three gradient-domain operations: sharpness saliency representation, affinity-based gradient transformation, and gradient-domain image reconstruction. Moreover, we also propose an evaluation method based on sharpness distribution for analyzing all sharpness enhancement approaches in respect of sharpness characteristics. By evaluating the sharpness distribution and comparing the visual appearance, we demonstrate the effectiveness of our sharpness enhancement approach.

Keywords Sharpness enhancement · Gradient-domain filter · Image sharpening

1 Introduction

Sharpness enhancement is an image processing technique which can adjust the sharpness characteristics of one image to produce a new sharper result. For decades, numerous image filters [1], which directly manipulate pixel values in spatial domain or modulate frequencies in frequency domain, have been developed to achieve sharpness enhancement. However, most of them cannot eliminate image noise effectively due to intensifying in all pixels synchronously. Adobe Photoshop [2], a popular commercial software for image processing, provides a sharpen filter for sharpness enhancement, but this sharpen filter is often accompanied by image noise. As shown in Fig. 1(b), the enhanced result of Photoshop's sharpen filter is severely degraded because of image noise. To obtain an enhanced result without noise, its another sharpen filter can only boost high-contrast regions by constructing an unsharp mask; however, the effectiveness of the unsharp mask filter depends on how accurately users set the given parameters. Since its unsharp mask can cause the incoherent sharpness enhancement in some local regions, it might fail to achieve the high-quality edge preserving. As shown in Fig. 1(c), although Photoshop's unsharp mask filter can eliminate image noise effectively, it cannot preserve the smooth edge feature due to the incoherent enhancement.

Later some optimization-based filters [3–5] are proposed, which can generate edge-preserving enhanced results by constructing a global optimization function and solving a large linear system, but they often introduce the halos artifacts and suffer from long computation time. Recently, two better image filters have been further proposed: based on bilateral filter [6], a guided filter [7] with O(N) time can efficiently enhance image sharpness and preserve smooth edge feature by a guidance image; another local Laplacian filter [8] can directly manipulate Laplacian pyramids for edge-aware image processing without degrading edges or introducing halos. However, these filters only focus on boosting all details synchronously. Thus they often produce unrealistic results because of immoderate enhancement in some local details. As we have seen in Figs. 1(d), 1(e), and 1(f),

Z.F. Xie (✉) · Y. Gui · M.G. Chen · L.Z. Ma
Shanghai Jiaotong University, Shanghai, China
e-mail: zhifeng_xie@sjtu.edu.cn

R.W.H. Lau
City University of Hong Kong, Kowloon, Hong Kong

Published online: 19 January 2012

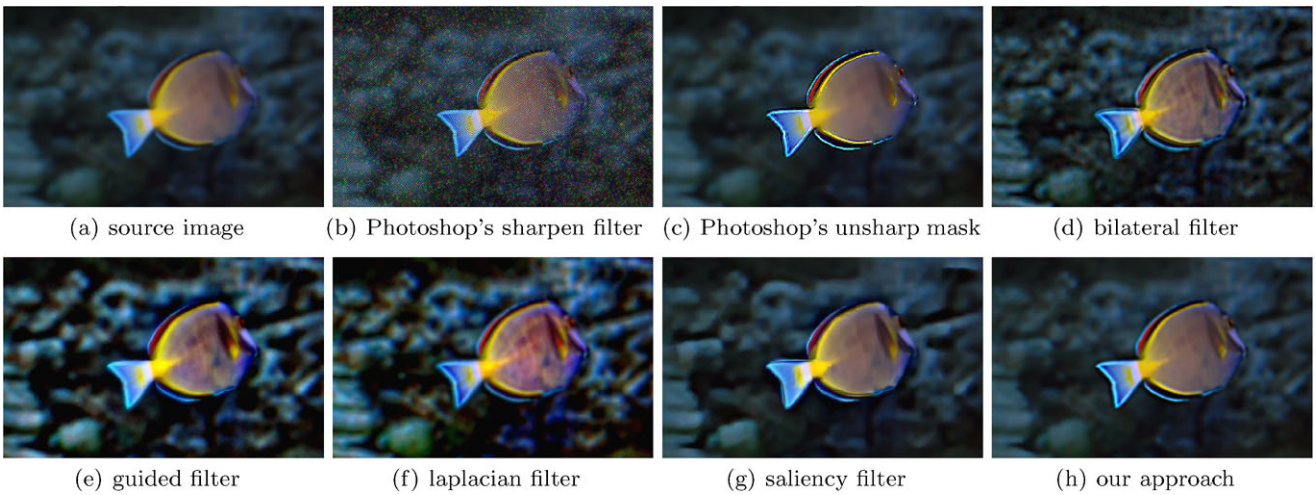

Fig. 1 Sharpness enhancement. (**a**) Source image. (**b**) The enhanced result of Photoshop's sharpen filter with boost 5 (*iters* = 5, i.e., it is performed five times iteratively). (**c**) The enhanced result of Photoshop's unsharp mask filter with boost 5 (*iters* = 5, *amount* = 200, *radius* = 1.0, *threshold* = 5). (**d**) The enhanced result of bilateral filter with boost 5 (*multiplier* = 5, $W = 5$, $\sigma_r = 3$ and $\sigma_s = 0.1$). (**e**) The enhanced result of guided filter with boost 5 (*multiplier* = 5, $r = 16$, $\epsilon = 0.01$). (**f**) The enhanced result of Laplacian filter with boost 5 ($\alpha = 0.2$, $\sigma_r = 0.4$, $\beta = 1$). (**g**) The enhanced result of saliency filter with boost 5 (*multiplier* = 5, *elNorm* = 1000, *pinchExp* = 5.0, *accuracy* = 1e−12, *maxIters* = 50, *maxLevels* = 2). (**h**) The enhanced result of our approach with boost 5 (*iters* = 5). Note: Unlike the Photoshop's sharpen filter and our approach, the other filters can provide more adjustable parameters, and their boost operations are also diverse

although these three filters can achieve the edge-preserving sharpness enhancement, they cannot still yield the high-fidelity enhanced results due to some unrealistic local details.

Apart from traditional filters in spatial and frequency domains, some gradient-domain filters [9, 10], which manipulate pixel differences in addition to pixel values of an image, also have been proposed for sharpness enhancement. Since they boost the pixel differences instead of direct manipulation in all pixels, the gradient-domain filters can maintain original features of the source image effectively. However, these filters might still suffer from image noise because of synchronous intensification in all gradients. The recent saliency sharpen filter [11] can use a long-edge detector to only enhance salient gradients without boosting image noise or background texture, but the incorrect long-edge detection might cause its failure to achieve the high-quality edge-preserving behavior. Like the Photoshop's unsharp mask filter, it might also generate the incoherent enhancement between long edges and local regions. As shown in Fig. 1(g), the saliency filter fails to produce a high-fidelity enhanced result with the smooth edge feature.

In this paper, we present a novel gradient-domain approach for sharpness enhancement, which can enhance the sharpness characteristics of source image with effective affinity-based edge preserving. On the one hand, since only local salient gradients in source image are selected into sharpness enhancement, our approach can avoid synchronous intensification. On the other hand, since affinity-based optimization can provide the smooth gradient transformation, our approach can also preserve the better edge feature. As shown in Fig. 1(h), compared with the other six filters, our edge-preserving sharpness enhancement approach can produce a high-fidelity enhanced result without image noise, unrealistic details, and incoherent enhancement.

In order to yield a sharper result with high-quality edge feature, our system pipeline shown in Fig. 2 includes three primary steps: sharpness saliency representation, affinity-based gradient transformation, and gradient-domain image reconstruction. First of all, we specify the pixels with local maximum gradient magnitude as salient pixels and represent the sharpness saliency by gradient paths each of which can pass through a corresponding salient pixel and trace along its gradient directions (two sides) pixel by pixel until the gradient magnitude does not decrease anymore. Secondly, we initialize the gradient transform ratio of each pixel in the gradient paths and obtain the smooth gradient transformation by optimizing an affinity-based energy function. Finally, guided by the new transformed gradients, we reconstruct a sharper result by minimizing another energy function with the constraints both in image domain and gradient domain. Moreover, since traditional verification of a sharpness enhancement approach is primarily based on visual appearance, which is often insufficient and inaccurate, we propose an efficient evaluation method based on sharpness distribution to further compare our approach with the other six filters.

In summary, our specific contributions in this paper are:

- A novel edge-preserving sharpness enhancement approach, which can effectively achieve the high-fidelity

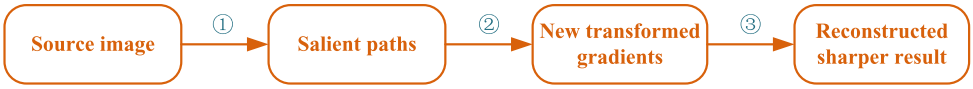

Fig. 2 Pipeline with three steps: (1) sharpness saliency representation; (2) affinity-based gradient transformation; (3) gradient-domain image reconstruction

enhancement in respect of sharpness characteristics by a pipeline with three gradient-domain operations.

- An effective evaluation method based on sharpness distribution, which can evaluate a sharpness enhancement approach accurately by analyzing the sharpness distribution in its enhanced output.

After a brief review of related work in next section, we elaborate our edge-preserving sharpness enhancement approach in Sect. 3. Our new evaluation method is introduced in Sect. 4. The related experiment results are shown in Sect. 5. A final conclusion and discussion about this paper are given in Sect. 6.

2 Related work

As the most fundamental operation of computer graphics and computer vision, image filtering allows users to apply various effects on images. A lot of image filters have been developed to enhance/modify/warp/mutilate images during the past few decades. In respect of sharpness enhancement, traditional methods [1], such as Laplacian filter, Sobel filter, ideal filter, butterworth filter, Gaussian filter, etc., can be divided into two categories: spatial-domain filters, which involve direct operation on image pixels, and frequency-domain filters, which involve the Fourier transform of one image for its operation. As a popular commercial software for image processing, Adobe Photoshop [2] also provided some sharpen filters to adjust the sharpness characteristics of one image. However, these previous filters often fail to produce a high-fidelity enhanced result with edge-preserving due to image noise or incoherent enhancement.

Later some optimization-based filters [3–5] were proposed for high-quality edge-preserving results. However, they often introduce the halos artifacts, and solving the corresponding linear system for optimization is time-consuming. Recently, based on bilateral filter [6], He et al. [7] proposed a new type of explicit image filter with O(N) time, called a guided filter. The guided filter, derived from a local linear model, can employ the input image itself or another different image as a guidance image and preserve better edge feature by considering the content of the guidance image. In addition, Paris et al. [8] also proposed a local Laplacian filter for edge-aware image processing, which can directly manipulate Laplacian pyramids to eliminate halos artifacts and preserve smooth edge feature. These two filters can be seamlessly applied to sharpness enhancement and achieve high-quality edge-preserving behavior. However, they focus on boosting all details synchronously and might generate the immoderate enhancement in some local details.

Unlike the spatial-domain and frequency-domain filters, the gradient-domain filters manipulate pixel differences in addition to pixel values of an image. In the past ten years, many gradient-domain filters have been successfully applied to a variety of image applications. Fattal et al. [12] proposed one of the first gradient-domain image filters to achieve the compression of HDR image. Perez et al. [13] constructed a guidance gradient field to create the seamless insertion of a source image patch into a target image. Levin et al. [14] used a similar gradient-domain filter to achieve seamless image stitching. They [15] also proposed a gradient-domain technique for stroke-based colorization. Lischinski et al. [16] improved Levin's gradient-domain technique to achieve interactive local tone adjustment. Orzan et al. [17] proposed a gradient-domain approach to convert photographs into abstract renditions. Agrawal et al. [18] used a gradient-based projection approach to integrate gradients for well-lit images without strong highlights. Agrawal et al. [19] involved this approach into image edge-suppressing operations. Later Agrawal et al. [20] further investigated robust surface reconstruction from a nonintegrable gradient domain. Zeng et al. [9] proposed a variational model with a data term in gradient-domain problems for image editing. Based on Zeng's work, Bhat et al. [10] achieved Fourier analysis of the 2D screened Poisson equation for gradient domain problems. Bhat et al. [11] also developed GradientShop to enable new image and video processing filters like saliency sharpening, suppressing block artifacts in compressed images, nonphotorealistic rendering, pseudo-relighting, and colorization. Recently, Ding et al. [21] implemented a novel interactive tool for image editing, and Xie et al. [22] improved the previous gradient-based methods for seamless video composition. Later Zhang et al. [23] further achieved an environment-sensitive image cloning technique.

In sharpness enhancement, Zeng et al. [9] first proposed a gradient-domain filter to sharpen an image. Their model interprets sharpness enhancement as a variational problem concerning adaptive adjustments of the zeroth and first derivatives of the images which correspond to the color and gradient items. Starting with Zeng's variational formulation, Bhat et al. [10] further generalized the Laplacian sharpen

filter by solving the 2D screened Poisson equation. Unfortunately, these approaches still intensify all gradients in an image and might fail to eliminate image noise. Later Bhat et al. [11] proposed a saliency sharpen filter which only intensifies those gradients that correspond to salient image features. The saliency filter uses a long-edge detector to boost those gradients that lie across long edges. Thus it can eliminate noise efficiently. However, the saliency filter might still fail in some situations due to the incorrect long-edge detection or incoherent enhancement between long edges and local details, which will cause that its enhanced result cannot preserve the high-quality edge feature. In this paper, in order to yield a high-fidelity enhanced result without image noise, unrealistic details, or incoherent enhancement, we propose a new edge-preserving approach for sharpness enhancement.

3 Edge-preserving sharpness enhancement

In this section, we introduce a novel pipeline to efficiently enhance the sharpness characteristics of source image. Figure 2 illustrates an overview of our edge-preserving sharpness enhancement approach, including sharpness saliency representation, affinity-based gradient transformation, and gradient-domain image reconstruction.

3.1 Sharpness saliency representation

Inspired by some gradient-domain edge priors [24, 25], we represent sharpness saliency accurately by gradient paths that pass through the pixels with local maximum gradient magnitude and trace along their gradient directions (two sides) pixel by pixel until the gradient magnitude does not decrease anymore. Based on this local representation, our sharpness enhancement can efficiently operate these gradient paths to avoid synchronous intensification in all gradients. Here, we define the pixels with local maximum gradient magnitude as salient pixels and also specify their corresponding gradient paths as salient paths.

Given an image I, we denote the gradient at each pixel $p = (x, y)$ as $\nabla I(p) = (\nabla I_x(p), \nabla I_y(p))$, where $\nabla I_x(p) = I(x+1, y) - I(x, y)$ and $\nabla I_y(p) = I(x, y+1) - I(x, y)$, and also define its gradient magnitude as $M(p) = \|\nabla I(p)\|$. First of all, we parameterize the ray in the gradient direction at each pixel by the following equation:

$$p^t = (x^t, y^t) = \begin{cases} x^t = x + t \cdot \nabla I_x(p)/M(p), \\ y^t = y + t \cdot \nabla I_y(p)/M(p), \end{cases} \quad (1)$$

where t is a regularization parameter. Then, starting from any pixel p, we find out its two neighbor pixels p^1 and p^{-1} in the gradient direction. If $M(p) > M(p^1)$ and $M(p) > M(p^{-1})$, we denote p as a salient pixel z_0 with local maximum gradient magnitude. Finally, after obtaining all salient pixels, we further construct each corresponding salient path by a recursive algorithm: (1) initialize a salient path $P(z_0)$ that can pass through the salient pixel z_0; (2) set an incremental variable i and a decremental variable j to zero; (3) add a forward neighbor pixel p_i^1, where p_i^1 is the $(i+1)$th pixel p_{i+1} along the positive gradient direction; (4) repeat step 3 until $M(p_{i+1}^1) > M(p_i^1)$; (5) add a backward neighbor pixel p_j^{-1}, where p_j^{-1} is the $|j-1|$th pixel p_{j-1} along the negative gradient direction; (6) repeat step 5 until $M(p_{j-1}^{-1}) > M(p_j^{-1})$; (7) define the final salient path as: $P(z_0) = (p_{-n}, \ldots, z_0, \ldots, p_m)$, where $m + n + 1$ is the number of gradients in the salient path. As shown in Fig. 3, we can find out all related salient pixels and initialize their corresponding salient paths by this representation method.

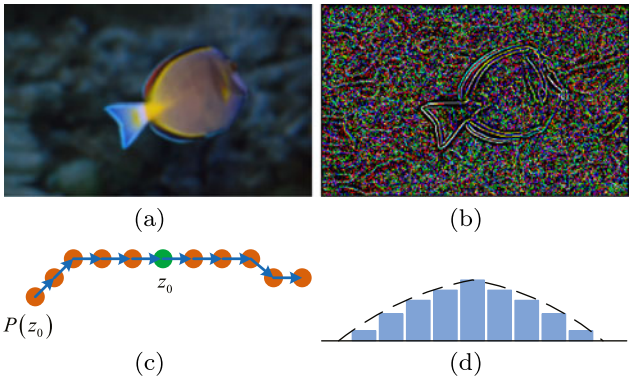

Fig. 3 Sharpness saliency representation. (**a**) Source image. (**b**) All salient pixels in source image. (**c**) The corresponding salient path $P(z_0)$ of a salient pixel z_0. (**d**) The gradient magnitude distribution in the salient path $P(z_0)$

According to the foregoing definition, the sharpness saliency in an image consists of all salient paths in the gradient domain. The steeper the gradient magnitude distribution in a salient path, the sharper the local saliency. This saliency representation will help to not only avoid the direct manipulation in all pixels but also carry out the asynchronous intensification in all gradients. In fact, our approach can exactly achieve the sharpness enhancement by adjusting these local gradient distributions in the salient paths.

3.2 Affinity-based gradient transformation

Based on sharpness saliency representation, we further transform gradients in the source image for sharpness enhancement. In this section, we first initialize a transform ratio map without synchronous intensification in all gradients. Then, to preserve high-quality edge feature, we optimize the transform ratio map by minimizing an affinity-based energy function. Finally, we utilize the final optimized ratio map to transform all gradients in the source image.

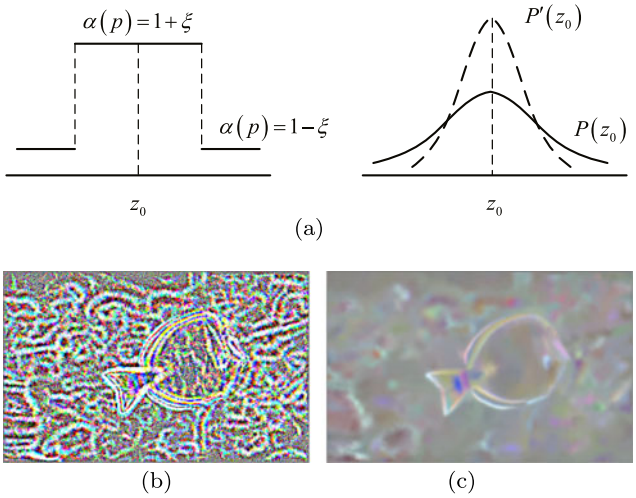

Fig. 4 Affinity-based gradient transformation. (**a**) Initialization of the gradient transform ratios in a salient path and the corresponding transformation of its gradient magnitude distribution. (**b**) The initial transform ratio map. (**c**) The optimized transform ratio map

Given a ratio interval $\xi \in [0, 1]$, we denote the gradient transform ratio as $\alpha(p) \in [1-\xi, 1+\xi]$ and define its new transformed gradient as $\nabla I'(p) = \alpha(p) \cdot \nabla I(p)$. As shown in Fig. 4(a), for each salient path $P(z_0) = (p_{-n}, \ldots, z_0, \ldots, p_m)$ in the source image, we first split it into three subsalient paths: $P_1 = (p_{-n/2}, \ldots, z_0, \ldots, p_{m/2})$, $P_2 = (p_{-n}, \ldots, p_{-(n+1)/2})$, and $P_3 = (p_{(m+1)/2}, \ldots, p_m)$. After that, we initialize $\{\alpha(p) = 1+\xi, p \in P_1\}$ and $\{\alpha(p) = 1-\xi, p \in P_2|P_3\}$. Finally, we can yield a new salient path $P'(z_0)$ with the steeper magnitude distribution, where each new gradient can be defined as $\nabla I'(p) = \alpha(p) \cdot \nabla I(p)$ using its corresponding gradient $\nabla I(p)$ and transform ratio $\alpha(p)$. By processing all salient paths, we can obtain a transform ratio map α^* in the source image. Obviously, as shown in Fig. 4(b), the asynchronous adjustment in all gradients can be achieved very well by the initial transform ratio map. However, since the discrete ratio map α^* does not consider the continuity between neighbor ratios, the new transformed gradients $\nabla I' = \alpha^* \cdot \nabla I$ cannot preserve the smooth edge feature sufficiently.

Therefore, in order to achieve high-quality edge-preserving, we construct the following affinity-based energy function with a smooth term and a data term to optimize the transform ratio map:

$$E(\alpha) = \sum_{i \in N} \sum_{j \in N} W_{ij}(\alpha_i - \alpha_j)^2 + \lambda \sum_{i \in N} (\alpha_i - \alpha_i^*)^2, \qquad (2)$$

where α is the optimized transform ratio map, α^* is the initial transform ratio map, N is the number of pixels in source image, λ is a regularization parameter, which is fixed to 1e−4, W refers to the popular matting affinity [26, 27]; here W_{ij} can be defined as

$$\sum_{k|(i,j)\in w_k} \left(\delta_{ij} - \frac{1}{|w_k|} \times \left(1 + (I_i - \mu_k)^T \left(\Sigma_k + \frac{\epsilon}{|w_k|} I_3\right)^{-1} (I_j - \mu_k)\right)\right), \qquad (3)$$

where I_i and I_j are the colors of the source image at pixels i and j, δ_{ij} is the Kronecker delta, μ_k and Σ_k are the mean and covariance matrix of the colors in the window w_k, I_3 is the 3×3 identity matrix, ϵ is a regularizing parameter, and $|w_k|$ is the number of pixels in the window w_k.

Finally, for minimizing the energy function $E(\alpha)$ and yielding the optimized transform ratio map α, we use the conjugate gradient method to solve the set of linear equations

$$(W + \lambda U)\alpha = \lambda \alpha^*, \qquad (4)$$

where U is the identity matrix. As shown in Fig. 4(c), compared with the initial transform ratio map, we can obtain the smoother ratio map by the affinity-based optimization. Due to the continuous ratio map α, the final transformed gradients $\nabla I' = \alpha \cdot \nabla I$ will not only avoid the synchronous intensification in all gradients but also generate the coherent sharpness enhancement.

In brief, as a most important step in our pipeline, the gradient transformation focuses on how to yield an ideal gradient transform ratio map for high-quality edge preserving. Here, it can be divided into two stages, initialization and optimization. In the first stage, we initialize a discrete transform ratio map according to the sharpness saliency representation. The purpose of the initialization is to adjust the gradient distribution in each salient path. In the second stage, we construct an affinity-based energy function to optimize the initial transform ratio map. The optimization aims to improve the continuity between new transformed gradients. Compared with the other filters, our sharpness enhancement with affinity-based gradient transformation can effectively suppress image noise and sufficiently preserve smooth edge feature.

3.3 Gradient-domain image reconstruction

Guided by the transformed gradients of source image, we next reconstruct a new enhanced image by minimizing an energy function with the constraints both in image domain and gradient domain. More specifically, the new reconstructed image can be associated with source image by an image-domain constraint; the gradients of new reconstructed image can also be associated with the transformed gradients of source image by a gradient-domain constraint.

(a) boost 1 (b) boost 3 (c) boost 5 (d) boost 7

Fig. 5 Illustration of our edge-preserving sharpness enhancement in iterations. (**a**)–(**d**) The enhanced results with boost 1, 3, 5, and 7, i.e., our pipeline is iteratively performed for a sharper output

Given a source image I and its transformed gradients $\nabla I' = \alpha \cdot \nabla I$, we can minimize the following energy function to generate a new reconstructed image:

$$E(\Phi) = \int_{p \in I} \|\nabla \Phi_p - \nabla I'_p\|^2 + \lambda |\Phi_p - I_p|^2 \, dp, \tag{5}$$

where Φ is the new reconstructed source image with its gradient and $\nabla \Phi$, and λ is a regularization parameter, which is set to 0.5 in this paper. Since this energy function is quadratic, its global optimum can be achieved by solving a set of linear equations. Here, as a numerical iterative algorithm, we use the conjugate gradient method to efficiently solve the following linear system:

$$\nabla^2 \Phi - \lambda \Phi = \nabla^2 I' - \lambda I, \tag{6}$$

where ∇^2 is the Laplacian operator, and $\nabla^2 I'$ is the divergence of transformed gradients $\nabla I'$. As shown in Fig. 5(a), after the image reconstruction in the gradient domain, our whole pipeline is completely performed to obtain a final enhanced result with high-quality edge preserving.

Often, as we have seen in Fig. 5, for a high-fidelity enhanced output, we need to iteratively boost an image by our novel pipeline with three gradient-domain operations until its sharpness characteristics can fully reach the required standard. In the interactive process, our approach will achieve the progressive sharpness enhancement, which can eliminate image noise, unrealistic details, and incoherent enhancement existed in the other filters.

4 Evaluation

At present, we can only verify a sharpness enhancement approach by our eyes, which causes that the evaluation in the visual appearance is insufficient. Therefore, in this section, to accurately compare our edge-preserving sharpness enhancement with the other six filters, we propose an efficient evaluation method based on sharpness distribution. For each sharpness enhancement approach, we calculate the sharpness distribution difference between its boosted result and ground truth. After that, we evaluate all sharpness enhancement approaches by comparing and analyzing their corresponding sharpness distribution differences.

First of all, we estimate the sharpness characteristics of one image by a measure equation based on salient path. Formally, given any salient path $P(z_0)$, we compute the sharpness $\Psi(P(z_0))$ of the salient path using the following measure equation:

$$\Psi(P(z_0)) = \int_{p \in P(z_0)} \frac{M(p)}{N} \cdot \|p - z_0\|^2 \, dp, \tag{7}$$

where $N = \sum_{p \in P(z_0)} M(p)$ is the sum of all gradient magnitudes in the salient path $P(z_0)$. Obviously, this measure equation indicates that the steeper the gradient magnitude distribution in the salient path, the smaller the sharpness value. After calculating the corresponding sharpness values of all salient paths, we can further yield a sharpness distribution Ψ^I in the specified image I.

Then, we can calculate the sharpness distribution difference between two images with different sharpness characteristics. Given two sharpness distributions Ψ^{I_1} and Ψ^{I_2}, we compute their sharpness means and standard deviations (μ_1, σ_1) and (μ_2, σ_2), and estimate their sharpness distribution difference using the following equation:

$$d(\Psi^{I_1}, \Psi^{I_2}) = \|\boldsymbol{\nu}_1 - \boldsymbol{\nu}_2\|, \tag{8}$$

where d is the Euclidean distance between two vectors $\boldsymbol{\nu}_1 = (\mu_1 - c \cdot \sigma_1, \mu_1 + c \cdot \sigma_1)$ and $\boldsymbol{\nu}_2 = (\mu_2 - c \cdot \sigma_2, \mu_2 + c \cdot \sigma_2)$, $\boldsymbol{\nu}_1$ and $\boldsymbol{\nu}_2$ indicate the upper and lower bounds of sharpness distributions in two images, and c is a constant which is often fixed to 1. Equation (8) indicates that the closer two sharpness distributions are, the smaller d is. Here, for each sharpness enhancement approach, we need to calculate the sharpness distribution difference between each boosted result and its ground truth.

Finally, we further compare and analyze the corresponding sharpness distribution differences of all sharpness enhancement approaches. As shown in Figs. 6 and 7(a), we provide all enhanced results of the seven approaches between boost 1 and boost 5, and also compute their sharpness distribution differences by (7) and (8). According to

Fig. 6 Comparison. (**a**) Source image. (**b**) Its ground truth with sharpness enhancement. (**c**) The enhanced results of these seven approaches with boost 1 (Photoshop's sharpen filter and Photoshop's unsharp mask filter: *iters* $= 1$; bilateral filter and guided filter: *multiplier* $= 1$; Laplacian filter: $\alpha = 1$; saliency filter: *multiplier* $= 1$; our approach: *iters* $= 1$). (**d**) Their enhanced results with boost 2 (Photoshop's sharpen filter and Photoshop's unsharp mask filter: *iters* $= 2$; bilateral filter and guided filter: *multiplier* $= 2$; Laplacian filter: $\alpha = 0.8$; saliency filter: *multiplier* $= 2$; our approach: *iters* $= 2$). (**e**) Their enhanced results with boost 3 (Photoshop's sharpen filter and Photoshop's unsharp mask filter: *iters* $= 3$; bilateral filter and guided filter: *multiplier* $= 3$; Laplacian filter: $\alpha = 0.6$; saliency filter: *multiplier* $= 3$; our approach: *iters* $= 3$). (**f**) Their enhanced results with boost 4 (Photoshop's sharpen filter and Photoshop's unsharp mask filter: *iters* $= 4$; bilateral filter and guided filter: *multiplier* $= 4$; Laplacian filter: $\alpha = 0.4$; saliency filter: *multiplier* $= 4$; our approach: *iters* $= 4$). (**g**) Their enhanced results with boost 5 (Photoshop's sharpen filter and Photoshop's unsharp mask filter: *iters* $= 5$; bilateral filter and guided filter: *multiplier* $= 5$; Laplacian filter: $\alpha = 0.2$; saliency filter: *multiplier* $= 5$; our approach: *iters* $= 5$)

Sharpness distribution difference	Source image	Boost 1	Boost 2	Boost 3	Boost 4	Boost 5
Photoshop's sharpen filter [2]	1.45	1.15	0.84	0.62	0.67	0.91
Photoshop's unsharp mask filter [2]	1.45	1.36	1.22	1.14	1.11	1.10
Bilateral filter [6]	1.45	1.03	0.95	0.88	0.85	0.83
Guided filter [7]	1.45	1.44	1.53	1.52	1.51	1.50
Laplacian filter [8]	1.45	1.45	1.49	1.59	1.69	1.67
Saliency filter [11]	1.45	0.97	0.91	0.90	0.91	0.92
Our approach	1.45	1.43	1.08	0.76	0.53	0.39

(a)

Run-time performance	Elapsed time (s)	Implementation platform
Photoshop's sharpen filter [2]	<1	/
Photoshop's unsharp mask filter [2]	<1	/
Bilateral filter [6]	39.45	Matlab
Guided filter [7]	1.48	Matlab
Laplacian filter [8]	1773	Matlab
Saliency filter [11]	56	C++
Our approach	2.85	C++

(b)

Fig. 7 Evaluation. (**a**) Sharpness distribution difference between the ground truth and each boosted result of seven approaches: Photoshop's sharpen filter, Photoshop's unsharp mask filter, bilateral filter, guided filter, Laplacian filter, saliency filter, and our sharpness enhancement. (**b**) Run-time performance comparison of these approaches

the variations in sharpness distribution difference, we can analyze each sharpness enhancement approach: (1) Photoshop's sharpen filter fails to eliminate image noise, which causes that its sharpness distribution differences are first decreased and later increased. (2) Photoshop's unsharp mask filter only enhances some high-contrast regions by constructing a unsharp mask, which causes that its sharpness distribution differences are decreased slowly after boost 2. (3) The bilateral filter smoothes the image while preserving edges by a weighted average of neighboring pixels, which causes that the variations in its sharpness distribution difference are decelerated after boost 2. (4) The guided filter employs the source image itself as a guidance image and considers its content to preserve edge feature, which causes that its sharpness distribution differences are always stable from boost 1 to boost 5. (5) The Laplacian filter focuses on synchronous detail enhancement with edge preserving, which causes that its sharpness distribution difference are not decreased effectively. (6) The saliency filter only boosts in the salient gradients using a long-edge detector, which causes that its sharpness distribution differences are almost fixed after boost 1. (7) Our approach can achieve an efficient sharpness enhancement with affinity-based edge preserving, which causes that its sharpness distribution differences are always decreased from boost 1 to boost 5. Compared with the other six filters, our approach can not only get a minimum sharpness distribution difference but also produce a high-fidelity enhanced result that approximates to the ground truth in the visual appearance. In summary, we believe that our edge-preserving sharpness enhancement is superior to the other filters in respect of offering the optimal sharpness distribution.

Moreover, to improve the run-time performance of our approach, we accelerate our pipeline by an O(N)-time algorithm [7] for affinity-based gradient transformation and an FFT-based screened Poisson solver [10] for gradient-domain reconstruction. After that, we choose Fig. 6(a) (800×600) as a common test case and experiment the running time of each approach in a laptop with a 2.1-Hz Intel Core 2 Duo CPU and a 4-Gb Memory. As shown in Fig. 7(b), we compare all approaches in the run-time performance: Photoshop's sharpen filter and unsharp mask filter have the outstanding running speed by some unknown techniques. In the Matlab platform, the comparison of their run-time performances is as follows: the guided filter $>$ the bilateral filter $>$ the Laplacian filter. As two gradient-domain approaches, the saliency filter and our sharpness enhancement are implemented in the C++ platform. Due to introducing the acceleration techniques, our approach has a better performance than the saliency filter.

5 Experiment results

In this section, we verify our edge-preserving sharpness enhancement approach on a variety of images and compare it

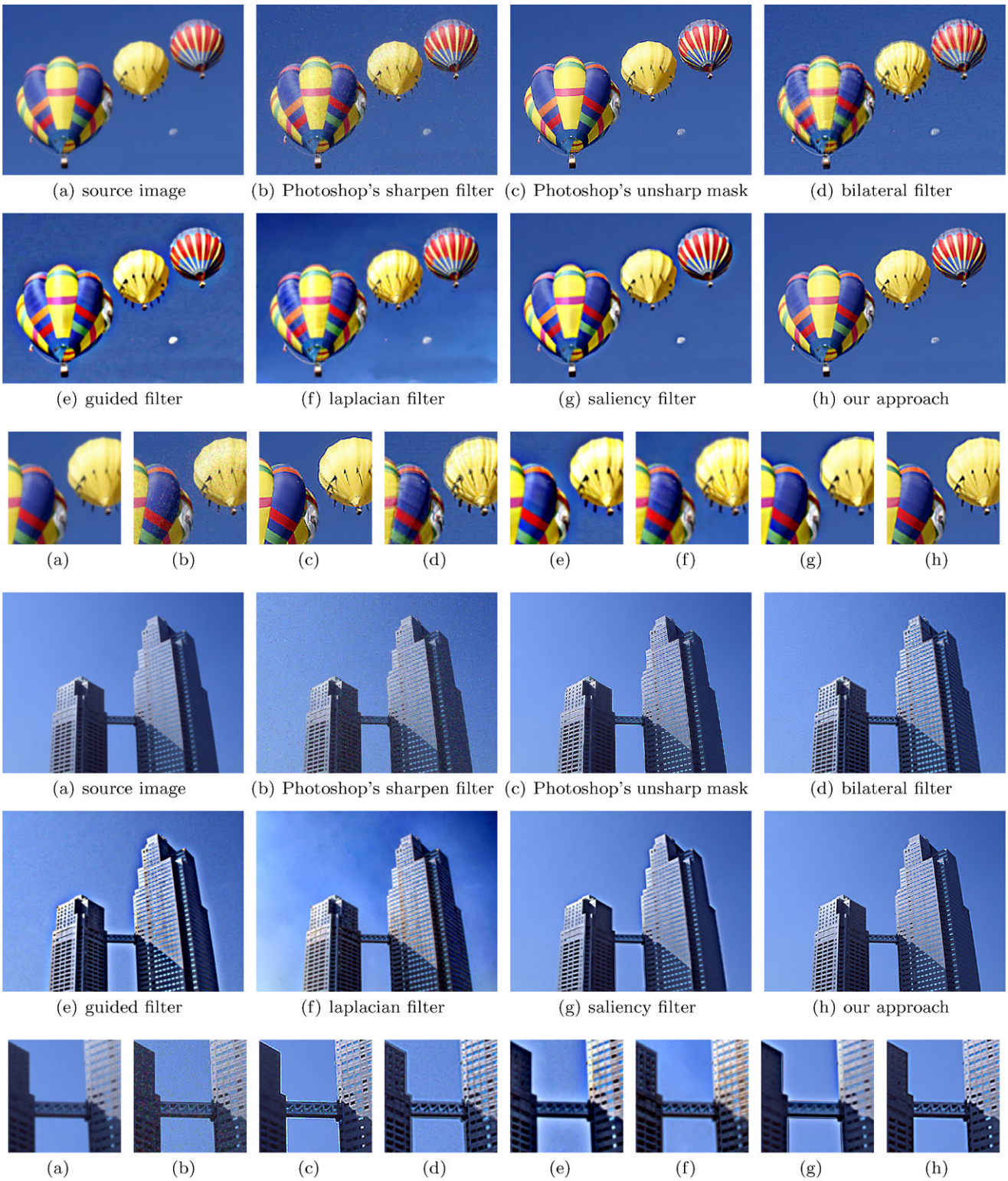

Fig. 8 Global sharpness enhancement with boost 5. (**a**) Source image. (**b**)–(**h**) The enhanced results of Photoshop's sharpen filter, Photoshop's unsharp mask filter, bilateral filter, guided filter, Laplacian filter, saliency filter, and our approach. Compared with the other six filters, our edge-preserving sharpness enhancement approach can yield the high-fidelity enhanced results without image noise, unrealistic details, and incoherent enhancement

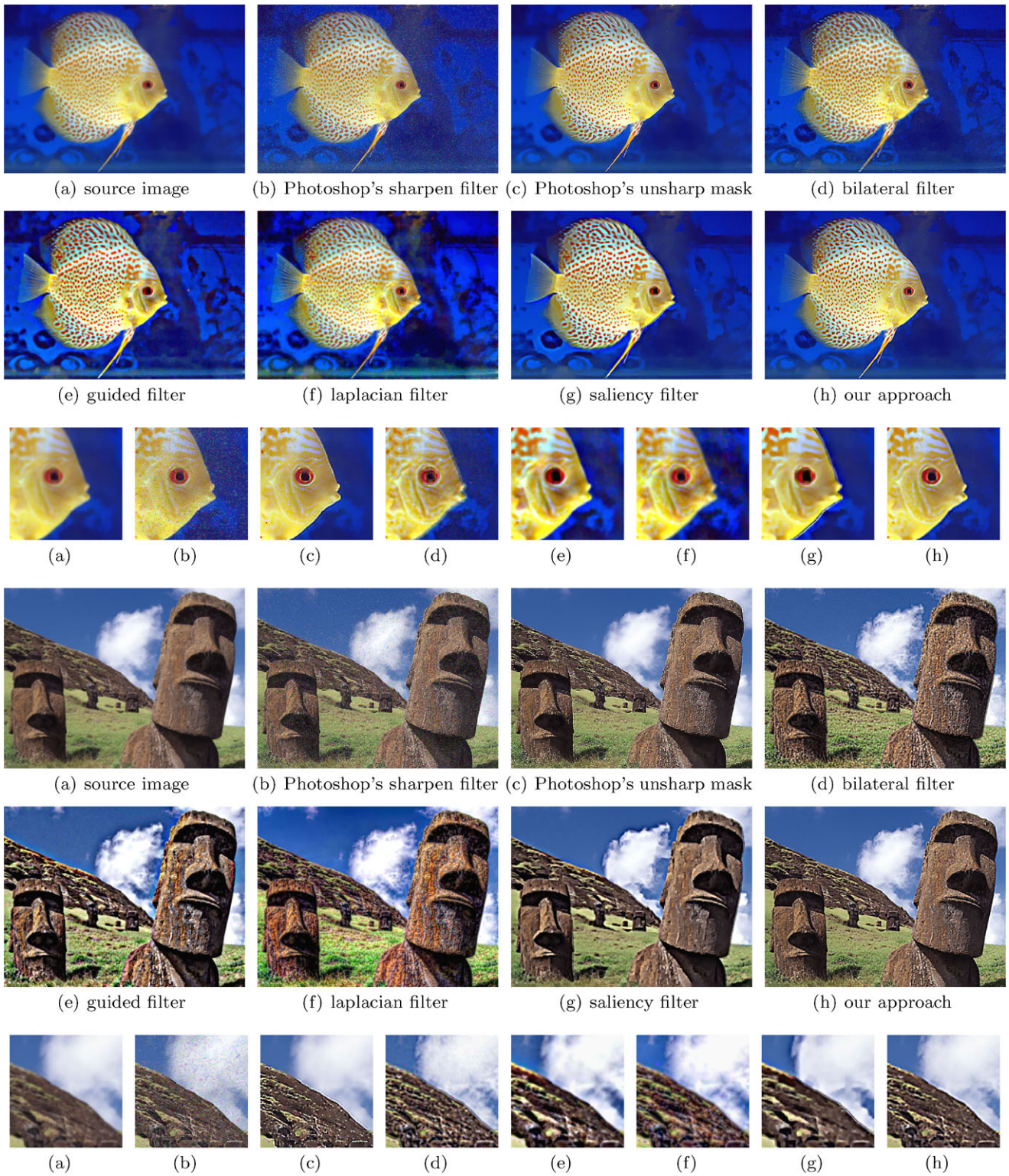

Fig. 9 Global sharpness enhancement with boost 5. (**a**) Source image. (**b**)–(**h**) The enhanced results of Photoshop's sharpen filter, Photoshop's unsharp mask filter, bilateral filter, guided filter, Laplacian filter, saliency filter, and our approach. Compared with the other six filters, our edge-preserving sharpness enhancement approach can yield the high-fidelity enhanced results without image noise, unrealistic details, and incoherent enhancement

with the other six filters (Photoshop's sharpen filter, Photoshop's unsharp mask filter, bilateral filter, guided filter, Laplacian filter, and saliency filter) in the visual appearance.

5.1 Global sharpness enhancement

Global sharpness enhancement can sharpen the whole region of one image. At present, most of traditional approaches often fail to produce the high-fidelity enhanced results due to image noise, unrealistic details or incoherent enhancement. On the contrary, our approach can enhance the sharpness characteristics of one image with affinity-based edge preserving, which can avoid or eliminate those artifacts existed in the traditional approaches.

As shown in Figs. 8 and 9, Photoshop's sharpen filter [2] produces the enhanced results with image noise; Photoshop's unsharp mask filter [2] improves the results of the sharpen filter by providing an unsharp mask, but its enhanced results might still suffer from the incoherent enhancement in some local regions; the bilateral filter [6], the guided filter [7], and the Laplacian filter [8] can also eliminate image noise while preserving smooth edge feature, but their enhanced results are degraded by some unrealistic local details more or less; in the gradient-domain sharpness enhancement approaches, the saliency filter [11] can suppress image noise and avoid unrealistic details effectively, but its enhanced results might still be influenced by the incoherent enhancement between long edges and local details; unlike the other six filters, our approach can yield the high-fidelity enhanced results without image noise, unrealistic details, and incoherent enhancement.

5.2 Local sharpness enhancement

Based on global sharpness enhancement, we can further achieve local sharpness enhancement by prespecifying the local region of one image. In our system, we have developed a simple interactive tool to specify the local region. First of all, we use this tool to manually draw a region of interest in source image as the user-specified mask. Then, we enhance the local region in source image by our edge-preserving sharpness enhancement algorithm.

As shown in Fig. 10, by specifying a local region, we can only focus on the dog and ignore other background. However, we might fail to achieve seamless sharpness enhancement due to the crude boundary between the user-specified region and the rest. Therefore, for seamless sharpness enhancement, our system needs to introduce image segmentation and image matting techniques [26, 28–31] to specify more accurate regions.

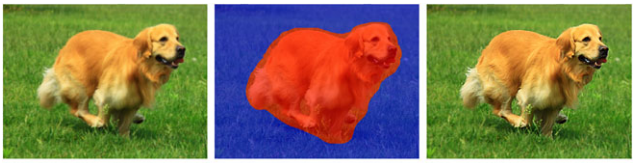

Fig. 10 Local sharpness enhancement. (**a**) Source image. (**b**) The user-specified mask. (**c**) The local enhanced result

6 Conclusion and discussion

In this paper, we propose a novel sharpness enhancement approach, which can yield a high-fidelity enhanced result by affinity-based edge preserving. In order to achieve the edge-preserving sharpness enhancement, we develop a new pipeline with three committed steps: sharpness saliency representation, affinity-based gradient transformation, and gradient-domain image reconstruction. Compared with the prevalent filters, our approach can efficiently eliminate image noise, unrealistic details, and incoherent enhancement. Moreover, we also propose an efficient evaluation method based on sharpness distribution, which can accurately evaluate each sharpness enhancement approach by comparing and analyzing the sharpness distribution difference between the boosted result and the ground truth. Apparently our approach can also be seamlessly applied to smooth an image when its gradient transformation is reversed. Thus, we have developed a new sharpness adjustment system, which not only provides image sharpening but also supports image smoothing.

As a future work, we are exploring other applications of our edge-preserving sharpness enhancement approach, including sharpness harmonization, image upsampling and image deblurring. However, one limitation of our method is that its run-time performance is not high enough to support real-time applications. We are exploring different acceleration techniques to speed up its performance. Another limitation of our method is that the user-specified masks are often deficient in local sharpness enhancement. We are currently also exploring some image segmentation and image matting algorithms for seamless sharpness enhancement.

Acknowledgements We would like to thank the anonymous reviewers for their valuable comments. This work was supported by the National Basic Research Project of China (No. 2011CB302203), the National Natural Science Foundation of China (No. 61073089, No. 61133009), the Innovation Program of the Science and Technology Commission of Shanghai Municipality (No. 10511501200), and a SRG grant from City University of Hong Kong (No. 7002664).

References

1. Gonzalez, R.C., Woods, R.E.: Digital Image Processing, 2nd edn. Addison-Wesley, Boston (2001)
2. Inc. Adobe, Systems. Photoshop CS 5, 2010
3. Elad, M.: On the origin of the bilateral filter and ways to improve it. IEEE Trans. Image Process. **11**, 1141–1151 (2002)
4. Farbman, Z., Fattal, R., Lischinski, D., Szeliski, R.: Edge-preserving decompositions for multi-scale tone and detail manipulation. ACM Trans. Graph. **27**, 67 (2008)
5. Fattal, R.: Edge-avoiding wavelets and their applications. ACM Trans. Graph. **28**(3), 1–10 (2009)
6. Tomasi, C., Manduchi, R.: Bilateral filtering for gray and color images. In: Proceedings of the Sixth International Conference on Computer Vision. ICCV '98, Washington, DC, USA, pp. 839–846. IEEE Computer Society, Los Alamitos (1998)
7. He, K., Sun, J., Tang, X.: Guided image filtering. In: Proceedings of the 11th European Conference on Computer vision: Part I, ECCV'10, pp. 1–14. Springer, Berlin (2010)
8. Paris, S., Hasinoff, S.W., Kautz, J.: Local Laplacian filters: edge-aware image processing with a Laplacian pyramid. In: ACM SIGGRAPH, SIGGRAPH '11, New York, NY, USA, 2011. ACM, New York (2011)
9. Zeng, X., Chen, W., Peng, Q.: A novel variational image model: towards a unified approach to image editing. J. Comput. Sci. Technol. 224–231 (2006)
10. Bhat, P., Curless, B., Cohen, M., Zitnick, C.L.: Fourier analysis of the 2d screened Poisson equation for gradient domain problems. In: Proceedings of the 10th European Conference on Computer Vision: Part II, pp. 114–128. Springer, Berlin (2008)
11. Bhat, P., Zitnick, C.L., Cohen, M., Curless, B.: Gradientshop: a gradient-domain optimization framework for image and video filtering. ACM Trans. Graph. **29**, 10:1–10:14 (2010)
12. Fattal, R., Lischinski, D., Werman, M.: Gradient domain high dynamic range compression. ACM Trans. Graph. **21**, 249–256 (2002)
13. Pérez, P., Gangnet, M., Blake, A.: Poisson image editing. ACM Trans. Graph. **22**, 313–318 (2003)
14. Levin, A., Zomet, A., Peleg, S., Weiss, Y.: Seamless image stitching in the gradient domain. In: Eighth European Conference on Computer Vision (ECCV 2004), pp. 377–389. Springer, Berlin (2003)
15. Levin, A., Lischinski, D., Weiss, Y.: Colorization using optimization. ACM Trans. Graph. **23**, 689–694 (2004)
16. Lischinski, D., Farbman, Z., Uyttendaele, M., Szeliski, R.: Interactive local adjustment of tonal values. ACM Trans. Graph. **25**, 646–653 (2006)
17. Orzan, A., Bousseau, A., Barla, P., Thollot, J.: Structure-preserving manipulation of photographs. In: Proceedings of the 5th International Symposium on Non-photorealistic Animation and Rendering, NPAR '07, New York, NY, USA, 2007, pp. 103–110. ACM, New York (2007)
18. Agrawal, A., Raskar, R., Nayar, S.K., Li, Y.: Removing photography artifacts using gradient projection and flash-exposure sampling. ACM Trans. Graph. **24**, 828–835 (2005)
19. Agrawal, A., Raskar, R., Chellappa, R.: Edge suppression by gradient field transformation using cross-projection tensors. In: Proceedings of the 2006 IEEE Computer Society Conference on Computer Vision and Pattern Recognition—vol. 2, CVPR '06, Washington, DC, USA, 2006, pp. 2301–2308. IEEE Computer Society, Los Alamitos (2006)
20. Agrawal, A., Raskar, R.: What is the range of surface reconstructions from a gradient field. In: ECCV, pp. 578–591. Springer, Berlin (2006)
21. Ding, M., Tong, R.f.: Content-aware copying and pasting in images. Vis. Comput. **26**(6–8), 721–729 (2010)
22. Xie, Z.-F., Shen, Y., Ma, L., Chen, Z.: Seamless video composition using optimized mean-value cloning. Vis. Comput. **26**(6–8), 1123–1134 (2010)
23. Zhang, Y., Tong, R.: Environment-sensitive cloning in images. Vis. Comput. **27**, 739–748 (2011)
24. Fattal, R.: Image upsampling via imposed edge statistics. ACM Trans. Graph. **26**(3), 95 (2007)
25. Sun, J., Xu, Z., Shum, H.-Y.: Image super-resolution using gradient profile prior. In: IEEE Conference on Computer Vision and Pattern Recognition, pp. 1–8 (2008)
26. Levin, A., Lischinski, D., Weiss, Y.: A closed-form solution to natural image matting. IEEE Trans. Pattern Anal. Mach. Intell. **30**, 228–242 (2008)
27. He, K., Sun, J., Tang, X.: Single image haze removal using dark channel prior. In: IEEE Computer Society Conference on Computer Vision and Pattern Recognition, pp. 1956–1963 (2009)
28. Boykov, Y.Y., Jolly, M.P.: Interactive graph cuts for optimal boundary & region segmentation of objects in N-D images. In: 8th IEEE International Conference on Computer Vision, vol. 1, pp. 105–112 (2001)
29. Rother, C., Kolmogorov, V., Blake, A.: Grabcut: interactive foreground extraction using iterated graph cuts. ACM Trans. Graph. **23**, 309–314 (2004)
30. Wang, J., Cohen, M.F.: Optimized color sampling for robust matting. In: IEEE Conference on Computer Vision and Pattern Recognition, 2007. CVPR '07, pp. 1–8 (2007)
31. He, K., Sun, J., Tang, X.: Fast matting using large kernel matting Laplacian matrices. In: IEEE Conference on Computer Vision and Pattern Recognition (2010)

Zhi-Feng Xie received the Master's degree from Department of Computer Science and Engineering of Jiangsu University, China in 2007. Now he is a Ph.D. candidate in Department of Computer Science and Engineering, Shanghai Jiao Tong University, China. His current research interests include image/video editing, computer vision, digital media technology.

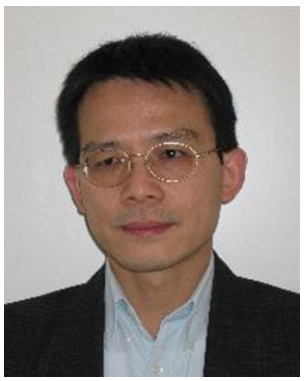

Rynson W.H. Lau received a (top) first-class B.Sc. honors degree in Computer Systems Engineering from the University of Kent, England, and a Ph.D. degree in Computer Science from the University of Cambridge, England. He has been on the faculty of Durham University, City University of Hong Kong, and The Hong Kong Polytechnic University. His research interests include Distributed Virtual Environments, Computer Graphics, and Multimedia Systems.

Yan Gui is a Ph.D. candidate of the Department of Computer Science and Technology, Shanghai Jiao Tong University, P.R. China. She received her B.Sc. and M.Sc. degrees in computer science in 2005 and 2008, both from Hunan Normal University and Central South University respectively. Her research interests include texture synthesis and image/video inpainting.

Min-Gang Chen received the Master's degree from East China Normal University, China in 2006. Now he is a Ph.D. candidate in Department of Computer Science and Engineering, Shanghai Jiao Tong University, China. His current research interests include image/video editing and digital media technology.

Li-Zhuang Ma received his B.Sc. and Ph.D. degrees at Zhejiang University, China in 1985 and 1991, respectively. He was a Post-doctor at the Department of Computer Science of Zhejiang University from 1991 to 1993. Dr. Ma was promoted as an Associative Professor and Professor in 1993 and 1995, respectively. Dr. Ma stayed at Zhejiang University from 1991 to 2002. He is now a Full Professor, Ph.D. Tutor, and the Head of Digital Media Technology and Data Reconstruction Lab at the Department of Computer Science and Engineering, Shanghai Jiao Tong University, China since 2002. He is also the Chairman of the Center of Information Science and Technology for Traditional Chinese Medicine at Shanghai Traditional Chinese Medicine University. Dr. Ma has published more than 100 academic research papers in both domestic and international journals. His research interests include computer-aided geometric design, computer graphics, scientific data visualization, computer animation, digital media technology, and theory and applications for computer graphics, CAD/CAM.